

## Probing the Outer Vestibule of a Sodium Channel Voltage Sensor

Naibo Yang,\* Alfred L. George, Jr.,# and Richard Horn\*

\*Department of Physiology, Institute of Hyperexcitability, Jefferson Medical College, Philadelphia, Pennsylvania 19107, and #Departments of Medicine and Pharmacology, Vanderbilt University School of Medicine, Nashville, Tennessee 37232 USA

**ABSTRACT** The second and third basic residues of the S4 segment of domain 4 (D4:R2 and D4:R3) of the human skeletal muscle Na<sup>+</sup> channel are known to be translocated from a cytoplasmic to an extracellular position during depolarization. Accessibilities of individual S4 residues were assayed by alteration of inactivation kinetics during modification of cysteine mutants by hydrophilic methanethiosulfonate reagents. The voltage dependences of the reaction rates are identical for extracellular application of cationic methanethiosulfonate-ethyltrimethylammonium (MTSET) and anionic methanethiosulfonate-ethylsulfonate (MTSES), suggesting that D4:R3C is situated outside the membrane electric field at depolarized voltages. The absolute rate of R3C modification is 281-fold greater for MTSET than for MTSES, however, suggesting that at depolarized voltages this S4 thiol resides in a negatively charged hydrophilic crevice. The two hydrophobic residues between D4:R2C and D4:R3C in the primary sequence (L1452 and A1453) are not externally exposed at any voltage. An  $\alpha$ -helical representation of D4/S4 shows that the basic residues D4:R2 and D4:R3 are on the face opposite that of L1452 and A1453. We propose that in the depolarized conformation, the hydrophobic face of this portion of D4/S4 remains in contact with a hydrophobic region of the extracellular vestibule of the S4 channel.

### INTRODUCTION

Activation of voltage-dependent ion channels, such as the Na<sup>+</sup>, K<sup>+</sup>, and Ca<sup>2+</sup> channels of nerve and muscle cells, requires the ability of charges to move across the membrane electric field in response to changes of membrane potential (Hodgkin and Huxley, 1952). The movements of these so-called gating charges are coupled to the opening and closing of the channels. Many voltage-dependent ion channels belong to a superfamily in which each of four subunits (in K<sup>+</sup> channels) or four homologous domains (in Na<sup>+</sup> and Ca<sup>2+</sup> channels) is composed of six putative transmembrane segments, S1–S6. The gating charges are believed to be concentrated primarily in the four positively charged S4 transmembrane segments of such channels. S4 segments must each transfer three to four elementary charges ( $e_0$ ) across the membrane electric field to account for the steep voltage dependence of gating of most Na<sup>+</sup> and K<sup>+</sup> channels (Schoppa et al., 1992; Zagotta et al., 1994; Hirschberg et al., 1995). The S4 segments in different ion channels contain from two to eight basic residues, either arginine or lysine, usually in a repetitive sequence in which positively charged residues are separated by two hydrophobic residues. Recent studies using cysteine scanning accessibility suggest a rather substantial reorientation of S4 residues in response to depolarization (Larsson et al., 1996; Mannuzzu et al., 1996; Yang et al., 1996). For example, two arginine residues of

the S4 segment of domain 4 (D4) of a human skeletal muscle Na<sup>+</sup> channel, specifically the second and third basic residues, R1451 and R1454 (which we denote as D4:R2 and D4:R3), are translocated from an internally accessible to an externally accessible location upon depolarization (Yang et al., 1996). Accessibility was determined by the reaction of two cysteine mutants, D4:R2C and D4:R3C, with the methanethiosulfonate reagents methanethiosulfonate-ethyltrimethylammonium (MTSET) and methanethiosulfonate-ethylsulfonate (MTSES). (In this paper the notation D4:R3C may signify either a specific amino acid residue or the channel containing this point mutation.) The covalent modification by these reagents causes a slowing of inactivation kinetics. We interpreted these results as evidence that in wild-type (WT) channels, D4:R2 and D4:R3 each transfer one positive charge completely across the membrane electric field in response to a depolarization.

Fig. 1 shows that this may be an overinterpretation. The S4 segment of D4 is depicted as a cylinder, with the cysteine residue R3C indicated. Depolarization causes an outward movement of D4/S4, shown here as an upward translocation, through an "S4 channel" (distinct from the pore that conducts Na<sup>+</sup> ions) that spans the hydrophobic core of the protein. The D4:R3C residue is accessible to MTSET and MTSES intracellularly at hyperpolarized voltages (*left panel*) and extracellularly at depolarized potentials (*right panel*). The right panel shows the membrane electric field subdivided into three regions: extracellular, intracellular, and core. The relative fractions of the electric field for these regions are  $\delta_{\text{ext}}$ ,  $\delta_{\text{int}}$ , and  $\delta_{\text{core}}$ , respectively. By definition, if the R3C residue is located anywhere in the extracellular or intracellular region, it is accessible to the hydrophilic cysteine reagents. Note that this exposure does not guarantee that R3C is completely outside the electric field. The residue may move as little as a fraction of  $\delta_{\text{core}}$  through the electric

Received for publication 25 April 1997 and in final form 2 July 1997.

Address reprint requests to Dr. Richard Horn, Department of Physiology, Thomas Jefferson University Medical College, 1020 Locust St., Philadelphia, PA 19107. Tel.: 215-503-6725; Fax: 215-503-2073; hornr@jefflin.tju.edu.

Dr. Yang's present address is Department of Molecular and Cellular Physiology, Stanford University School of Medicine, Beckman Center, Stanford, CA 94305.

© 1997 by the Biophysical Society  
0006-3495/97/11/2200/09 \$2.00

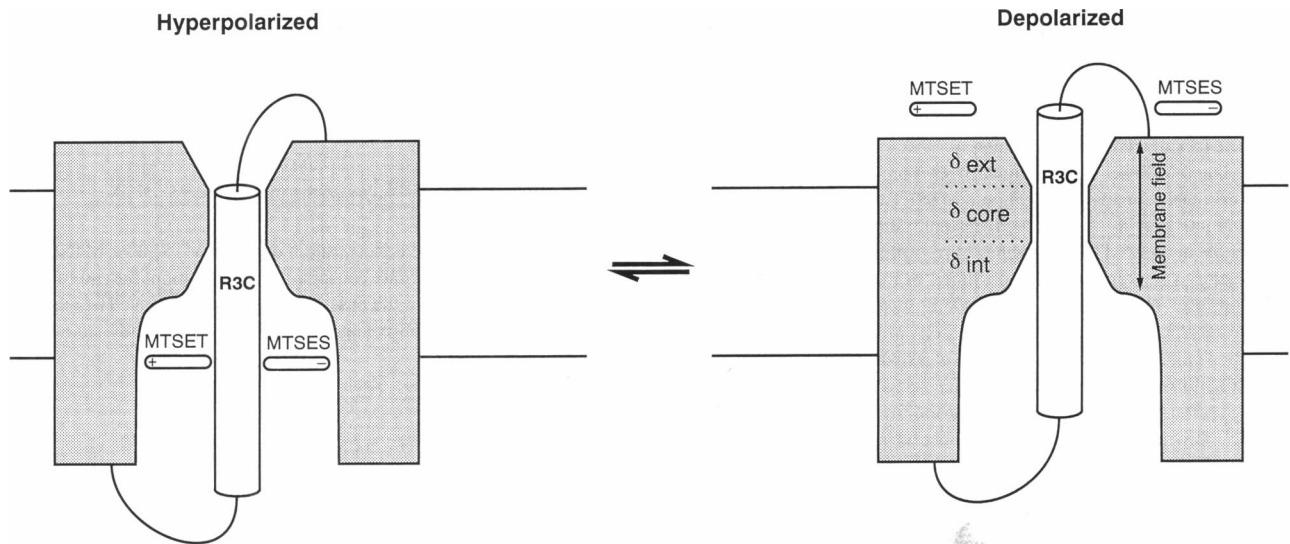


FIGURE 1 Schematic model of D4/S4 in its channel at hyperpolarized (*left*) and depolarized (*right*) voltages. Note the partition of the electric field into three separate fractions,  $\delta_{\text{ext}}$ ,  $\delta_{\text{int}}$ , and  $\delta_{\text{core}}$ . We define the core as the region inaccessible to MTS reagents. The magnitude of  $\delta_{\text{ext}}$  will be estimated as described in the text.

field during its translocation. If, for example,  $\delta_{\text{core}} = 0.5$ , the guanidinium moiety of the arginine residue R3 may traverse the hydrophobic core, carrying as little as  $0.5 e_0$ . The importance of this possibility is that there must be a quantitative agreement between the total gating charge movement per channel and that contributed by the putative voltage sensors. If charged residues in S4 traverse only a portion of the membrane electric field, it may be necessary to look elsewhere (e.g., the acidic residues in segments S2 and S3; Papazian et al., 1995; Seoh et al., 1996) for charged residues that contribute to gating.

Here we explore this issue by measuring the voltage dependence of D4:R3C exposure to both the cationic reagent MTSET and the anionic reagent MTSES (Fig. 1), using methods described previously (Yang and Horn, 1995; Yang et al., 1996). We previously interpreted the voltage dependence of the reaction of R3C with MTSET as a consequence solely of a voltage-dependent change in the conformation of D4/S4. If, however, the monovalently charged reagents, applied extracellularly, each move a fraction of  $\delta_{\text{ext}}$  through the membrane electric field to reach residue R3C, the apparent voltage dependence of R3C exposure will be different for MTSET than for MTSES. This follows from the fact that although depolarization exposes R3C, it tends to drive a cation like MTSET out of, and an anion like MTSES into, the electric field. The experiments reported here show, however, that these oppositely charged reagents, applied extracellularly, have an identical voltage dependence for R3C modification, suggesting that depolarization moves R3C completely out of the membrane electric field. Moreover, the 281-fold higher absolute reactivity of the cationic reagent is evidence that this S4 thiol resides in a negatively charged crevice at depolarized voltages.

We further explore the extracellular mouth of the S4 channel by determining the voltage dependence of the ac-

cessibilities of the hydrophobic leucine and alanine residues, L1452 and A1453, between D4:R2 and D4:R3. Because the flanking arginine residues are both translocated during a depolarization, we assume that L1452 and A1453 are likewise translocated. However, the introduced cysteine residues L1452C and A1453C are never accessible extracellularly, even at depolarized voltages, although they are accessible intracellularly at hyperpolarized voltages. We interpret this result as evidence that the section of D4/S4 encompassing these four residues has an  $\alpha$ -helical structure.

## MATERIALS AND METHODS

### Mutagenesis

The hSkM1 mutants R1448C (D4:R1C) and R1454C (D4:R3C) were constructed as described previously (Chahine et al., 1994; Yang et al., 1996). Mutants L1452C, A1453C, and G1456A were constructed in hSkM1, using a single-step polymerase chain reaction mutagenesis strategy (Higuchi, 1989). Primers were designed to create the desired mutation and incorporate natural restriction sites for *Hind*III (nt 4051) and *Sac*II (nt 4467) in the final product. Amplifications (20 cycles) were performed, using 20 ng of hSkM1 cDNA as template and *Taq* DNA polymerase. Final products were purified by spin-column chromatography (Qiagen, Chatsworth, CA), digested with *Hind*III and *Sac*II, and the resulting 416-bp fragment was ligated into the corresponding sites in the plasmid pRc/CMV-hSkM1. The amplified region was sequenced entirely in the final construct to verify the mutation and to exclude polymerase errors.

All mutant constructs were introduced into tsA201 cells, a transformed variant of HEK293 cells, by transient transfection (Yang et al., 1996). Cells were used for recording 40–80 h after transfection.

### Electrophysiology and data acquisition

Standard whole cell recording methods were used as previously described (Yang and Horn, 1995). Supercharging reduced the expected charging time constant for the cells to  $<10 \mu\text{s}$ . Series resistance errors were  $<3 \text{ mV}$ . Data were filtered at 5 kHz and were acquired with pCLAMP (Axon Instru-

ments, Burlingame, CA). Patch electrodes contained (in mM) 105 CsF, 35 NaCl, 10 EGTA, 10 Cs-HEPES (pH 7.4). The bath contained 150 NaCl, 2 KCl, 1.5 CaCl<sub>2</sub>, 1 MgCl<sub>2</sub>, 10 Na-HEPES (pH 7.4). Corrections were made for liquid junction potentials. Steady-state inactivation was measured by reduction in peak current at -20 mV, preceded by a 500-ms conditioning pulse. All experiments were performed at 18°C.

MTSET and MTSES were obtained from Toronto Research Chemicals (North York, ON, Canada). The cationic MTSET covalently attaches ethyl trimethylammonium to the reduced cysteine sulfhydryl via a disulfide bond, and the anionic MTSES attaches ethyl sulfonate. Aqueous stocks of these reagents were kept at 4°C and diluted in the bath solution immediately before use. The reagent solutions were presented to the cells with a macropipette placed in apposition to the cell. Macropipettes were pulled from 2-mm (O.D.) pyrex tubing after the glass was internally coated with sigmacote (Sigma, St. Louis, MO) to reduce surface tension. The macropipette length after pulling was 50 mm, and the tip diameter was ~30–100 μm. After the whole cell configuration was obtained, the cells were lifted ~200 μm off the surface of the dish. After the macropipette was filled, it was lowered into the bath. In its final position the opening was placed within 50 μm of the cell. Usually the gravity-induced outflow of the macropipette caused a visible distortion of the cell. The adequacy of solution exchange was confirmed in other experiments in which changes in extracellular Na<sup>+</sup> concentration reliably produced expected changes in the reversal potential of Na<sup>+</sup> current.

The cells were maintained at a holding potential of either -140 mV or -160 mV and were stimulated every 20 s or 30 s by a 20-ms test pulse to -20 mV, to measure inactivation kinetics. Effects of these reagents were irreversible in the absence of added reducing agents. In some experiments cysteine reagents were included in the patch pipette to modify channels from the cytoplasmic face of the channel protein in a whole cell recording. In this case the tip of the pipette was filled with reagent-free internal solution, and the pipette was then back-filled with reagent-containing solution. This procedure was necessary to avoid exposing the outside of the cells to reagent. The amount of reagent-free solution in the pipette tip was adjusted empirically so that the initial effects of the reagents were observed after a period of ~5 min after breaking into the cell.

Depolarizations were required for extracellular exposure of D4/S4 residues. For MTSET modification of D4:R3C, 10 depolarizations of 900 ms each were presented in the 20-s interval between brief test depolarizations to -20 mV. Between each these 10 depolarizations the voltage was returned to -140 mV for 900 ms. Therefore, the cells spent a total of 9 s at a depolarized potential and 11 s at the holding potential between test depolarizations. For MTSES modification of D4:R3C we used a single 9-s depolarization followed by an 11-s hyperpolarization to -160 mV. The latter protocol allowed complete recovery from slow inactivation induced by MTSES modification of D4:R3C channels (Yang et al., 1997).

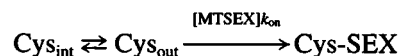
For modification of D4:R1C we used the same voltage protocol for MTSET and MTSES, a 10-s depolarization to +20 mV followed by a 10-s return to the -150 mV holding potential and a 20-ms test depolarization to -20 mV to measure inactivation kinetics. We applied either 20 μM MTSET or 150 μM MTSES and estimated the first-order modification rate as described previously (Yang and Horn, 1995). The second-order rate constant for modification was calculated from the first-order rate by dividing by the reagent concentration and multiplying by 2 to account for the 50% duty cycle of the depolarizations. We previously reported that doubling the concentration of MTSET doubled the rate of modification of D4:R1C (Yang and Horn, 1995), consistent with a bimolecular reaction. We further confirmed this result here, using MTSES on the same mutant (data not shown).

## Data analysis and modeling

Whole cell data were analyzed and displayed by a combination of pCLAMP programs, ORIGIN (MicroCal, Northampton, MA), and our own FORTRAN programs. Data from at least three cells for each measurement are presented as means ± SEM. To estimate parameters for Boltzmann functions, we either fit data from individual cells (steady-state inactivation), or used modification rates from individual cells, obtained from modification time constants (Yang and Horn, 1995).

tion), or used modification rates from individual cells, obtained from modification time constants (Yang and Horn, 1995).

We assume that D4:R3C is exposed externally in a voltage-dependent fashion, and that only the exposed residue is accessible to external reagent, as depicted in the following scheme:



[MTSEX] represents the concentration of either MTSET or MTSES,  $k_{\text{on}}$  is the pseudo-second-order rate constant for modification; the modification is considered irreversible in the absence of a reducing agent. The exposure of D4:R3C is assumed to be voltage dependent, with a steady-state exposure probability of

$$P_{\text{out}} = \frac{1}{1 + \exp(q(V_{\text{mid}} - V)/RT)}$$

where  $V$  is the depolarized membrane potential used to expose R3C,  $q$  is the effective number of S4 charges that move during external exposure of R3C,  $V_{\text{mid}}$  is the voltage at which half the D4/S4 segments are in an outward configuration, and  $RT/F = 24$  mV.

To account for the possibility that the cysteine residue D4:R3C moves a fraction of  $\delta_{\text{ext}}$  within the electric field when exposed by depolarization (Fig. 1), we assume that the rate of cysteine modification is proportional to

$$P_{\text{out}} \exp\left(\frac{-z\delta_{\text{ext}}VF}{RT}\right) \quad (1)$$

where  $z$  is the valence of the MTS reagent (either +1 or -1).

The parameters of Eq. 1 were estimated by a variable metric algorithm from the sum of squares of differences between the rates obtained from individual cells and the theoretical function. For speed and accuracy, partial derivatives of Eq. 1 with respect to the parameters were determined analytically, and asymptotic standard errors of the best estimates were based on the inverse of the Fisher information matrix. The estimates of  $\delta_{\text{ext}}$  were constrained to be between 0 and 1. We also used Eq. 1 to simultaneously fit the data for both MTSET and MTSES. In this case the parameters  $q$ ,  $V_{\text{mid}}$ , and  $\delta_{\text{ext}}$  were assumed to be the same for MTSET and MTSES.

Fig. 6 was created from an  $\alpha$ -helical model of D4/S4 by Graphicae (Philadelphia, PA).

## RESULTS

### Comparison of MTSET and MTSES modification of R3C

The mutant D4:R3C has biophysical properties that are similar, but not identical, to those of the WT channel hSkM1 (Fig. 2, A and B; see also Yang et al., 1996). Both cationic MTSET and anionic MTSES slow the inactivation kinetics of R3C. Fig. 2, C and D, shows Na<sup>+</sup> currents of the R3C mutant after complete modification by these reagents. The modification reaction requires, for both reagents, that the cell be depolarized to expose the introduced cysteine residue. Although both reagents markedly slow inactivation and reduce its voltage dependence, MTSES has a greater effect on the voltage dependence of the inactivation kinetics. This is also seen in steady-state inactivation measurements, where both reagents cause a depolarizing shift in the  $h_{\infty}$  curves (Fig. 3), but MTSES produces a greater reduction in the slope. Perhaps the most striking difference between the effects of these two reagents on R3C, however, is that

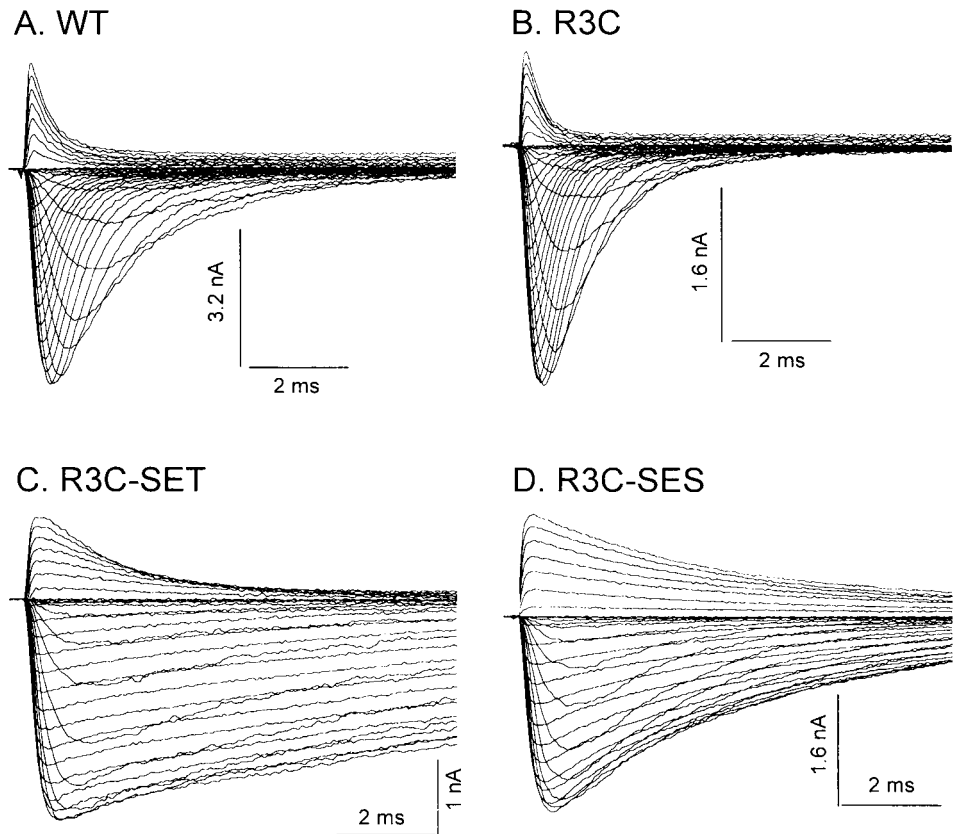


FIGURE 2 Whole cell currents and effects of MTS reagents on D4:R3C. Currents in A–C were elicited from –140 mV to test potentials between –80 and +70 mV in 5-mV increments. In D, the holding potential was –160 mV. (A) WT; (B) D4:R3C; (C) D4:R3C after modification by external 100  $\mu$ M MTSET; (D) D4:R3C after modification by external 5 mM MTSES.

MTSET-modified channels recover from inactivation  $\sim$ 30-fold faster than MTSES-modified channels (Yang et al., 1997). Because of the slow recovery from inactivation after MTSES modification, we used a highly negative holding potential (–160 mV) in all experiments using R3C and MTSES (see Materials and Methods). This allowed us to

observe the inactivation kinetics of all of the channels, which was necessary to obtain an unambiguous estimate of the modification rate.

Fig. 4 A shows the time course of modification of a cell by 5 mM MTSES. The initial exposure to MTSES had no effect on this cell when brief (20 ms) test pulses to –20 mV were applied every 20 s from the –160 mV holding potential (traces 1 and 2). However, when the cell was depolarized to a conditioning voltage of –100 mV during the 20-s intervals between test pulses (see inset above Fig. 4 A), the inactivation kinetics began to change, as a slow component replaced the rapidly inactivating component. Fig. 4 A shows the gradual change in the inactivation kinetics for modification, which was complete within  $\sim$ 7 min. These data show that the residue R3C is accessible to extracellular MTSES only when the channel is depolarized, in this example to –100 mV, in agreement with our previous results using MTSET (Yang et al., 1996).

During modification the inactivation kinetics were fit by a weighted sum of two exponential relaxations, fast for unmodified and slow for MTSES-modified channels. The rate of the MTSES reaction, estimated from the fractional weight of the slow component of inactivation, has exponential kinetics with a rate that increases as the conditioning voltage is made more positive (Fig. 4 B, open circles). The modification rates of R3C by 100  $\mu$ M MTSET, approximately scaled to these data, are plotted in Fig. 4 B (filled squares). The data for MTSET ( $n = 33$  cells) and for

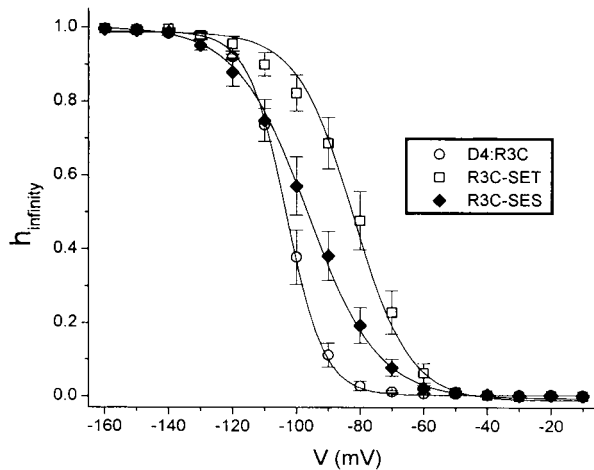


FIGURE 3 Steady-state inactivation for D4:R3C before and after modification by either MTSET or MTSES. Theory curves are fits to the Boltzmann equation, with midpoints of  $-103.1 \pm 1.8$  mV (R3C),  $-82.0 \pm 3.4$  mV (R3C-SET),  $-96.4 \pm 3.6$  mV (R3C-SES), and slopes of  $4.03 \pm 0.38 e_0$  (R3C),  $2.71 \pm 0.17 e_0$  (R3C-SET),  $2.16 \pm 0.11 e_0$  (R3C-SES).

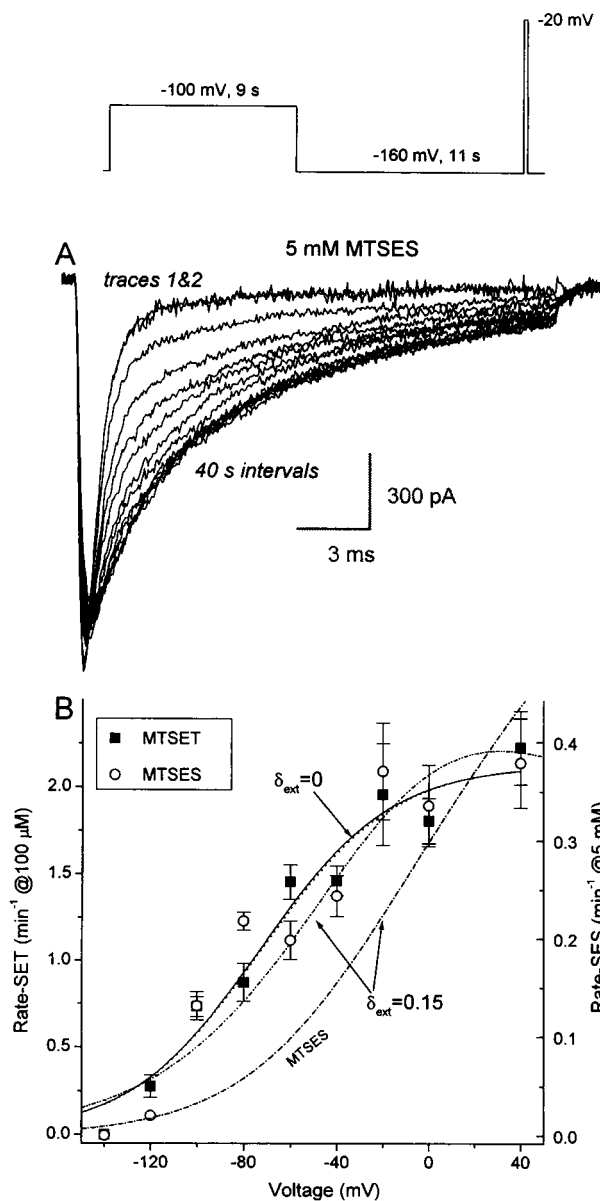


FIGURE 4 Rate and voltage dependence of modification of D4:R3C. (A) Modification by MTSES. Cell depolarized to  $-100$  mV for 9 s, then hyperpolarized to  $-160$  mV for 11 s, before measuring inactivation kinetics at  $-20$  mV (voltage protocol shown above). Every other current is shown. Traces 1 and 2 were obtained in the presence of MTSES, but in the absence of the depolarization to  $-100$  mV; no modification of inactivation was observed in the absence of depolarization. The rate of appearance of a slow time constant of inactivation is plotted in B for  $100 \mu\text{M}$  MTSET ( $\blacksquare$ ) and  $5 \text{ mM}$  MTSES ( $\circ$ ). Some of the data for MTSET modification were previously published (Yang et al., 1996). The ordinates for the data for the two reagents are scaled to correspond as closely as possible. The theory curves (—, MTSET; ···, MTSES) are best fits to a Boltzmann equation, with estimated parameters given in the text. The dash-dot lines represent theory from the best fit of all of the data for both reagents to Eq. 1, with  $\delta_{\text{ext}}$  fixed at 0.15. The lower dash-dot line at negative voltages shows expected rates for MTSES.

MTSES ( $n = 25$  cells) were individually fit by a Boltzmann function representing the probability  $P_{\text{out}}$  of R3C exposure (see Materials and Methods). Each fit used three free pa-

rameters: a maximum rate, a midpoint, and a "slope" corresponding to  $q$ , the apparent charge moved during D4/S4 translocation. For MTSET the estimated midpoint was  $-73.0 \pm 7.5$  mV and the slope was  $0.90 \pm 0.19 e_0$ . For MTSES the estimated midpoint was  $-72.3 \pm 11.1$  mV and the slope was  $0.89 \pm 0.28 e_0$ . The theoretical curves corresponding to these fits are nearly superimposed and are indicated as  $\delta_{\text{ext}} = 0$  in Fig. 4 B (MTSET: solid line; MTSES: dotted line). Although the absolute rates of modification by these two reagents are quite different, as evident from the differential scaling of the ordinates of Fig. 4 B, the midpoints and slopes are not significantly different. Because MTSET is a cation and MTSES is an anion, these results suggest that R3C, when accessible to these reagents, is not situated within the membrane electric field.

We also fit the data for both reagents simultaneously, assuming in this case that exposure of R3C was independent of the reagent used. We therefore estimated a common midpoint and slope for the voltage dependence of exposure of R3C and a single free parameter ( $\delta_{\text{ext}}$ ) for the fractional electrical distance of the exposed R3C within the membrane electric field (see Eq. 1 in Materials and Methods). The value of  $\delta_{\text{ext}}$  was constrained to be between 0 and 1. The midpoint and slope for this fit were  $-73.1 \pm 5.2$  mV and  $0.89 \pm 0.13 e_0$ , respectively, and the estimate of  $\delta_{\text{ext}}$  was 0. To see the effect of forcing  $\delta_{\text{ext}}$  to be small, but finite, we fit all of the data simultaneously with a model (Eq. 1) in which  $\delta_{\text{ext}}$  was fixed at 0.15. The best fit theory curves for this model are plotted in Fig. 4 B (dash-dot lines). The discrepancy between theory and data is obvious, especially for MTSES (the lower theoretical curve at negative voltages), and lends credence to the conclusion that R3C is situated completely out of the membrane electric field at depolarized voltages.

### Intrinsic electrostatic potentials in D4/S4's outer vestibule

Fig. 4 B shows that D4:R3C, when exposed, reacts more rapidly with MTSET than with MTSES, even though we used a 50-fold higher concentration of MTSES. After correction for this concentration difference and the 45% duty cycle used in the depolarizations, a second-order rate constant can be estimated for each reagent from the maximum estimated rates in Fig. 4 B. These rate constants are  $793 \text{ M}^{-1} \text{ s}^{-1}$  (for MTSET) and  $2.82 \text{ M}^{-1} \text{ s}^{-1}$  (for MTSES). Therefore when D4:R3C is exposed extracellularly, MTSET modifies it 281-fold faster than MTSES. This may be compared with the relative reactivities of these two reagents for free thiols in solution.  $\beta$ -Mercaptoethanol, for example, also reacts more rapidly with MTSET than MTSES (Stauffer and Karlin, 1994). However, at the ionic strength of our bath solution (164 mM), the second-order rate constant for MTSET modification of  $\beta$ -mercaptoethanol is only 7.1-fold faster than that for MTSES. If we assume that the difference in relative reactivities of the S4

thiol and  $\beta$ -mercaptoethanol is due solely to long-range electrostatics, we can estimate an intrinsic electrostatic potential  $\Phi_{R3C}$  at D4:R3C as follows (Stauffer and Karlin, 1994; Cheung and Akabas, 1997).

The ratio of relative reactivities of D4:R3C and  $\beta$ -mercaptoethanol is  $\rho = 281/7.1 = 39.3$ . This ratio of ratios factors out the extent of ionization of the respective thiols due to the local environment (Stauffer and Karlin, 1994), and the electrostatic potential at R3C is then determined as

$$\Phi_{R3C} = -\frac{RT}{2F} \ln(\rho) = -45.9 \text{ mV}$$

This indicates that there is a substantial negative potential experienced by the S4 thiol, even though the local electric field is screened by mobile ions in the bath solution. Similar results were obtained for native cysteine residues in the vicinity of the acetylcholine binding site of a nicotinic receptor, although the estimated potential was only about  $-30$  mV at a lower ionic strength than we used (Stauffer and Karlin, 1994).

We used the same procedure to estimate an electrostatic potential for D4:R1C at a depolarized voltage ( $+20$  mV), where this cysteine residue is maximally exposed (Yang and Horn, 1995). These experiments yielded second-order rate constants for the modification of  $1944 \pm 154 \text{ M}^{-1} \text{ s}^{-1}$  (MTSET,  $n = 5$  cells) and  $88.5 \pm 5.8 \text{ M}^{-1} \text{ s}^{-1}$  (MTSES,  $n = 4$  cells). In this case the relative reactivity for D4:R1C and  $\beta$ -mercaptoethanol is  $\rho = 22.0/7.1 = 3.1$ , yielding an estimated electrostatic potential of  $-14.0$  mV. The larger negative potential obtained for R3C than for R1C supports a model in which D4/S4 residues, when exposed extracellularly by depolarization, reside in a charged hydrophilic crevice (see Discussion).

### Voltage-dependent accessibility of L1452C and A1453C

The voltage-dependent translocation of both D4:R2 and D4:R3 strongly suggests that the hydrophobic residues between them, L1452 and A1453 (see primary amino acid sequence at the top of Fig. 5), are also translocated upon depolarization. To test this we made a cysteine mutant of each and examined the effects of both internal and external cysteine reagents. To our surprise, neither mutant appeared to be modified during a 10-min external application of either  $100 \mu\text{M}$  MTSET or  $5 \text{ mM}$  MTSES under either depolarizing ( $0$  mV) or hyperpolarizing ( $-140$  mV) conditions. This has one of two explanations. Either the substituted cysteines are inaccessible to external reagent at any voltage, or the modification has no obvious biophysical consequence. The latter explanation is not valid, because both L1452C and A1453C react readily with internally applied MTSES, which slows inactivation kinetics (Fig. 5). These results, therefore, indicate that L1452C and A1453C are not exposed externally at voltages where R2C and R3C are both exposed.

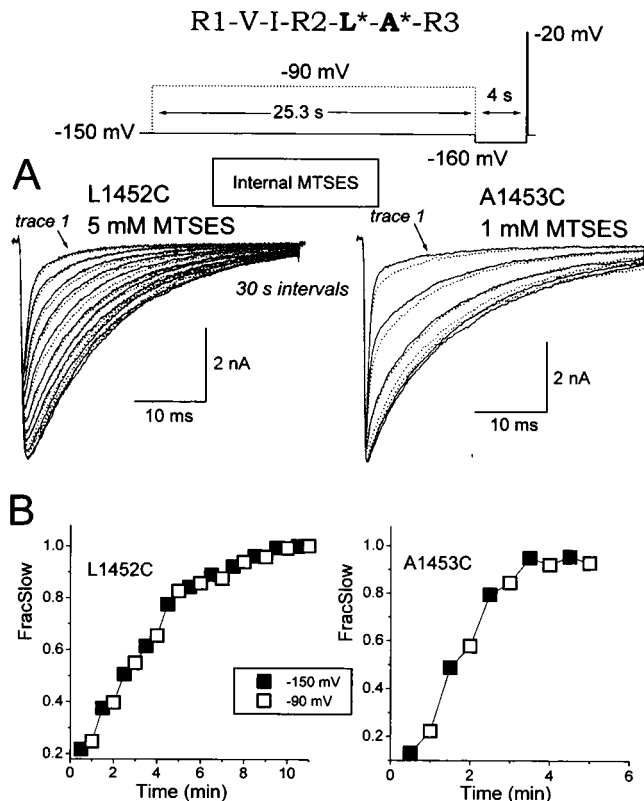


FIGURE 5 Modification by internal MTSES of L1452C and A1453C in whole cell recording. The amino acid sequence of this region of D4/S4 is shown above, with the substituted amino acids starred. The alternating voltage protocol is shown below this, and the corresponding currents for two representative cells are shown in A. (A) The dotted lines represent currents at the  $-20$  mV test pulse after the  $-90$ -mV conditioning potential, and solid lines represent the currents after the  $-150$ -mV conditioning potential. Modification occurs more rapidly after the  $-150$ -mV conditioning voltage, indicating that at  $-90$  mV these residues are poorly accessible to internal MTSES. (B) The fractional weight of the slower exponentially decaying component is plotted as a function of time for the currents depicted in A. This weight grows more slowly after depolarization to  $-90$  mV ( $\square$ ).

The outward translocation of both D4:R2 and D4:R3 upon depolarization makes it unlikely that the hydrophobic residues between them always remain in an intracellular location, leading to the prediction that modification of L1452C and A1453C can occur only at hyperpolarized voltages. To test this in our whole cell recordings, where reagent diffuses into the cell from the patch pipette, we used the voltage protocol shown above Fig. 5 A. A 20-ms test pulse to  $-20$  mV was applied every 30 s, and the intervening holding potential was alternated between  $-90$  and  $-150$  mV. To recover from inactivation induced at  $-90$  mV, we preceded each test pulse by a 4-s hyperpolarization to  $-160$  mV. Reaction with internal MTSES decreased the rate of inactivation; this occurred more rapidly after the  $-150$ -mV holding potential (Fig. 5 A, solid traces). This is especially obvious for the A1453C mutant. To quantify the time course of modification for the cells shown in Fig. 5 A, we fit the current decay as a sum of two exponential

components and plotted the fractional weight of the slow component (representing modified channels) in Fig. 5 B. In correspondence with the qualitative appearance of the current traces, the modification was slower after depolarizations to  $-90$  mV (*open squares*) than after holding the cells at  $-150$  mV (*filled squares*).

These results show that even a modest depolarization to  $-90$  mV is sufficient to make these two residues relatively inaccessible to MTSES, indicating a rather steep voltage dependence of D4/S4 movement. In contrast, the fits of the voltage dependence of external exposure of R3C (Fig. 4 B) suggest that at  $-90$  mV this residue is externally exposed only 35% of the time. We believe, however, that the movement of D4/S4 has a greater voltage dependence for the L1452C and A1453C mutants than for the R3C mutant, which could explain why the mutants of hydrophobic residues have a larger apparent voltage dependence of disappearance from the cytoplasmic compartment. The rationale for this argument is that the R3C mutation neutralizes an S4 residue that is likely to be important for S4 movement. This mutation is therefore expected to produce a decrease in the voltage sensitivity for movement of D4/S4, whereas the L1452C and A1453C mutations do not significantly change the charge of this S4 segment.

How can the lack of reaction of the L1452C and A1453C mutants to external reagents be explained? If D4/S4 has an  $\alpha$ -helical conformation, D4:R2 and D4:R3 lie on the face of the helix opposite that of the residues L1452 and A1453. Therefore, when D4/S4 is translocated outward upon depolarization, the hydrophobic face of this section of D4/S4 may remain in contact with a hydrophobic region at the external mouth of the S4 channel, while exposing D4:R2 and D4:R3. Fig. 6 depicts an  $\alpha$ -helical model of D4/S4 in a hyperpolarized (above) and depolarized (below) conformation within the putative S4 channel. At the hyperpolarized voltage, the D4/S4 residues from R2 through R8, including L1452 (*red*) and A1453 (*orange*), are accessible internally (Yang et al., 1996). Depolarization causes the movement of D4/S4 into and through its hydrophobic channel. At a depolarized voltage R1 through R3 are in an extracellularly accessible location. However, the hydrophobic residues L1452 and A1453 remain in contact with an external hydrophobic region in the mouth of the S4 channel. This model suggests, therefore, an  $\alpha$ -helical structure for a short region of D4/S4 at depolarized voltages.

## DISCUSSION

The modification of D4:R3C has a voltage dependence for the cationic reagent MTSET that is identical to its voltage dependence for the anion MTSES over the voltage range of  $-140$  to  $+40$  mV, suggesting that in WT channels the residue D4:R3 carries its positive charge completely out of the electric field during a depolarization. In terms of the cartoon in Fig. 1, this indicates that  $\delta_{\text{ext}} = 0$ . We have not examined the voltage dependence of the reaction of R3C

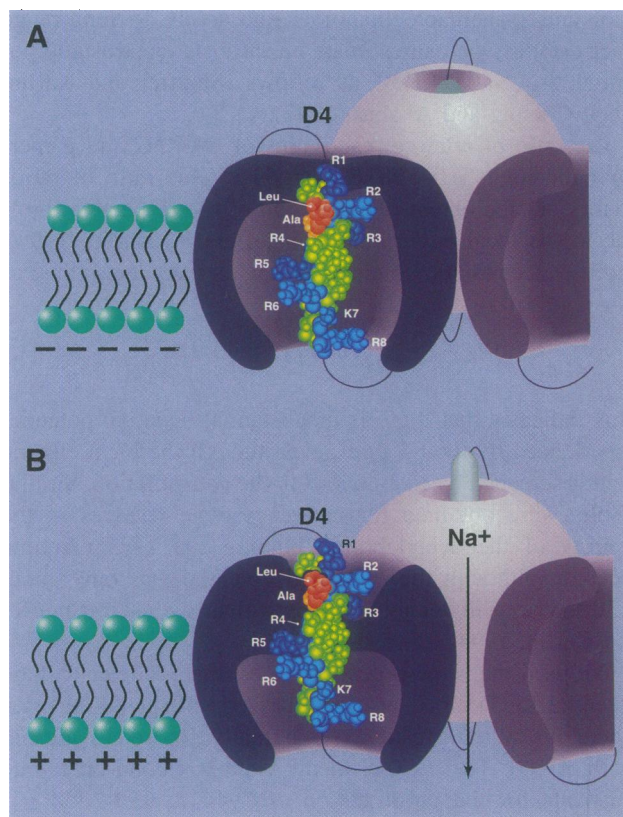


FIGURE 6 Model of D4/S4 movement. An  $\alpha$ -helical S4 structure is depicted, showing the change in accessibility of S4 residues at hyperpolarized (A) and depolarized (B) voltages. Note that although D4:R2 and D4:R3 are exposed extracellularly at depolarized voltages, the hydrophobic residues between them in the primary sequence are not. Our recent data (unpublished) indicate that the internal accessibilities of D4:R4 and D4:R5 are reduced at depolarized voltages, as shown. The accessibility of D4:R6 at a depolarized voltage is under study.

with intracellular cysteine reagents. However, it may be argued that because both R2C and R3C are accessible intracellularly at hyperpolarized voltages, R3C is likely to assume a more superficial position with respect to the electric field (Fig. 1). Although this is only a conjecture, our results are consistent with the idea that the residue D4:R3 in WT channels translocates its positive charge completely across the membrane electric field, and that all of this charge may therefore be coupled to the gating of the channel.

This satisfying conclusion ignores, however, the physical dimensions of these methanethiosulfonate reagents, which are  $\sim 7$  Å in length. Furthermore, the charged part of the molecule is at the opposite end of the reactive methanethiosulfonate part. It is conceivable, therefore, that the reactive part may enter the electric field to modify the exposed cysteine residue, leaving the charged part of the reagent out of the electric field (Fig. 1). If the external portion of the electric field falls across a distance of only a few angstroms, the reaction of an "exposed" cysteine to these reagents could be voltage independent, even though the exposure might not carry the cysteine completely out of the electric field. An alternative position to this argument is that the WT

arginine has a side chain  $\sim 4 \text{ \AA}$  longer than that of cysteine, and may therefore extend even farther from the hydrophobic core of the protein. Despite this ambiguity, our data suggest that at depolarized voltages R3C is either fully extended into the outer hydrophilic milieu at the external surface of the protein or is lying in a vestibule with a dielectric constant much larger than that of the protein core.

The large intrinsic electrostatic potential at R3C ( $\Phi_{\text{R3C}} = -46 \text{ mV}$ ) is difficult to reconcile, however, with a full exposure of this residue at depolarized voltages. Moreover, the low absolute values for reaction rates with R3C suggest the possibility of some geometric constraints in the access of this residue to MTS reagents. If  $\Phi_{\text{R3C}}$  is caused by negative charges near R3C, the number of elementary charges can be estimated by using a Poisson-Boltzmann formalism. For example, the screened Coulomb potential at distance  $r$  from a point source with a valence of  $z$  is given by (Moore, 1972)

$$\Phi = \frac{ze_0}{4\pi\epsilon_0\epsilon} \left( \frac{b}{1+br} \right)$$

where  $\epsilon_0$  is the permittivity of free space,  $\epsilon = 78.5$  is the dielectric constant of the aqueous solution, and  $b^{-1} = 7.4 \text{ \AA}$  is the Debye length in solution. Equating this potential with  $\Phi_{\text{R3C}}$  and solving for  $z$  gives an estimate of  $\sim 6$  negative charges at a reaction radius of  $10 \text{ \AA}$  from the thiol moiety of cysteine. It is difficult to imagine so much negative charge so near R3C if this residue is fully surrounded by a region of high dielectric potential. A more likely possibility is that R3C is situated within a hydrophilic crevice formed by the low-dielectric walls of the protein. This configuration will tend to enhance and "focus" the negative charge contributed by anionic side chains of residues within the crevice. A similar situation has been demonstrated for the active sites of superoxide dismutase enzymes, where potentials on the order of  $100 \text{ mV}$  are obtained (Getzoff et al., 1983; Desideri et al., 1992). These electrostatic potentials are larger for locations deeper within the active site. Similarly for the D4/S4 vestibule, the electrostatic potential at R1C is much smaller than at R3C, suggesting that R1C lies more superficially when D4/S4 is extended outward at depolarized membrane potentials (Fig. 6). An intriguing possibility is that the negative electrostatic potential in the outer vestibules of S4 segments contributes to the "surface potential" experienced by the voltage sensors in this superfamily of ion channels (Hille, 1992).

### Structure of the S4 segment

The secondary structure of S4 segments is unknown, although an  $\alpha$ -helical structure has been postulated (Catterall, 1986; Durell and Guy, 1992). Our results with L1452C and A1453C suggest that at least a short stretch of D4/S4 is  $\alpha$ -helical at depolarized voltages. At hyperpolarized voltages we know that basic residues from D4:R2 through D4:R8 (with the possible exception of the lysine residue

D4:K8; Yang et al., 1996), L1452, and A1453 are internally accessible, suggesting that a long stretch of D4/S4 is largely unconstrained by surrounding protein. We can only speculate on the structure of this region, but if it has an  $\alpha$ -helical conformation, the known exposed residues would wrap completely around it (Fig. 6). It is notable that the residue D4:R4 is preceded by a glycine residue (G1456), which has a low propensity for forming a helical structure (O'Neill and DeGrado, 1990). However, the residue with the strongest  $\alpha$ -helical potential, alanine, when substituted for this glycine residue, has little effect on inactivation (data not shown), again lending credence to the possibility that D4/S4 has a helical structure, both in depolarized and hyperpolarized conformations.

These data shed no light, however, on the conformation of D4/S4 during charge translocation. Although this transmembrane segment may maintain a rigid helical conformation during its voltage-dependent conformational changes, it is also possible that the transition involves uncoiling and recoiling of an  $\alpha$ -helix (Guy and Conti, 1990; Aggarwal and MacKinnon, 1996).

We thank Dr. Arthur Karlin for suggesting the calculation of intrinsic electrostatic potential and for a number of entertaining conversations about the vagaries of MTS reagents, Dr. Gregory Filatov for help with the molecular modeling in Fig. 6, and Dr. Nenad Mitrovic for comments on the manuscript.

Supported by National Institutes of Health grants AR41691 (RH) and NS32387 (ALG).

### REFERENCES

- Aggarwal, S. K., and R. MacKinnon. 1996. Contribution of the S4 segment to gating charge in the *Shaker* K<sup>+</sup> channel. *Neuron*. 16:1169–1177.
- Catterall, W. A. 1986. Molecular properties of voltage-sensitive sodium channels. *Annu. Rev. Biochem.* 55:953–985.
- Chahine, M., A. L. George, Jr., M. Zhou, S. Ji, W. Sun, R. L. Barchi, and R. Horn. 1994. Sodium channel mutations in paramyotonia congenita uncouple inactivation from activation. *Neuron*. 12:281–294.
- Cheung, M., and M. H. Akabas. 1997. Locating the anion-selectivity filter of the cystic fibrosis transmembrane conductance regulator (CFTR) chloride channel. *J. Gen. Physiol.* 109:289–299.
- Desideri, A., M. Falconi, F. Polticelli, M. Bolognesi, K. Djinović, and G. Rotilio. 1992. Evolutionary conservativeness of electric field in the Cu, Zn superoxide dismutase active site. *J. Mol. Biol.* 223:337–342.
- Durell, S. R., and H. R. Guy. 1992. Atomic scale structure and functional models of voltage-gated potassium channels. *Biophys. J.* 62:238–247.
- Getzoff, E. D., J. A. Tainer, P. K. Weiner, P. A. Kollman, J. Richardson, and D. C. Richardson. 1983. Electrostatic recognition between superoxide and copper, zinc superoxide dismutase. *Nature*. 306:287–290.
- Guy, H. R., and F. Conti. 1990. Pursuing the structure and function of voltage-gated channels. *Trends Neurosci.* 13:201–206.
- Higuchi, R. 1989. Using PCR to engineer DNA. In PCR Technology. H. A. Erlich, editor. Stockton Press, New York. 61–70.
- Hille, B. 1992. Ionic Channels of Excitable Membranes. Sinauer Associates, Sunderland, MA. 457–470.
- Hirschberg, B., A. Rovner, M. Lieberman, and J. Patlak. 1995. Transfer of twelve charges is needed to open skeletal muscle Na<sup>+</sup> channels. *J. Gen. Physiol.* 106:1053–1068.



- Hodgkin, A. L., and A. F. Huxley. 1952. A quantitative description of membrane current and its application to conduction and excitation in nerve. *J. Physiol.* 117:500–544.
- Larsson, H. P., O. S. Baker, D. S. Dhillon, and E. Y. Isacoff. 1996. Transmembrane movement of the *Shaker* K<sup>+</sup> channel S4. *Neuron.* 16:387–397.
- Mannuzzu, L. M., M. M. Moronne, and E. Y. Isacoff. 1996. Direct physical measure of conformational rearrangement underlying potassium channel gating. *Science.* 271:213–216.
- Moore, W. J. 1972. *Physical Chemistry*. Prentice-Hall, Englewood Cliffs, NJ. 453–454.
- O'Neill, K. T., and W. F. DeGrado. 1990. A thermodynamic scale for the helix-forming tendencies of the commonly occurring amino acids. *Science.* 250:646–651.
- Papazian, D. M., X. M. Shao, S.-A. Seoh, A. F. Mock, Y. Huang, and D. H. Wainstock. 1995. Electrostatic interactions of S4 voltage sensor in *Shaker* K<sup>+</sup> channel. *Neuron.* 14:1293–1301.
- Schoppa, N. E., K. McCormack, M. A. Tanouye, and F. J. Sigworth. 1992. The size of gating charge in wild-type and mutant *Shaker* potassium channels. *Science.* 255:1712–1715.
- Seoh, S. A., D. Sigg, D. M. Papazian, and F. Bezanilla. 1996. Voltage-sensing residues in the S2 and S4 segments of the *Shaker* K<sup>+</sup> channel. *Neuron.* 16:1159–1167.
- Stauffer, D. A., and A. Karlin. 1994. Electrostatic potential of the acetylcholine binding sites in the nicotinic receptor probed by reactions of binding-site cysteines with charged methanethiosulfonates. *Biochemistry.* 33:6840–6849.
- Yang, N., A. L. George, Jr., and R. Horn. 1996. Molecular basis of charge movement in voltage-gated sodium channels. *Neuron.* 16:113–122.
- Yang, N., A. L. George, and R. Horn. 1997. Probing the outer mouth of the “S4 channel” of a voltage-gated sodium channel. *Biophys. J.* 72:A262 (Abstr.).
- Yang, N., and R. Horn. 1995. Evidence for voltage-dependent S4 movement in sodium channels. *Neuron.* 15:213–218.
- Zagotta, W. N., T. Hoshi, J. Dittman, and R. W. Aldrich. 1994. *Shaker* potassium channel gating. II. Transitions in the activation pathway. *J. Gen. Physiol.* 103:279–319.